RESEARCH ARTICLE

Bone Marrow–Derived Gr1^{+} Cells Can Generate a Metastasis-Resistant Microenvironment Via Induced Secretion of Thrombospondin-1

Raúl Catena[1,2,3], Nandita Bhattacharya[4,5], Tina El Rayes[1,2,3], Suming Wang[4,5], Hyejin Choi[1,2,3], Dingcheng Gao[1,2,3], Seongho Ryu[1,2,3], Natasha Joshi[1,2,3], Diane Bielenberg[4,5], Sharrell B. Lee[1,2,3], Svein A. Haukaas[6,7], Karsten Gravdal[6], Ole J. Halvorsen[6], Lars A. Akslen[6], Randolph S. Watnick[4,5], and Vivek Mittal[1,2,3]

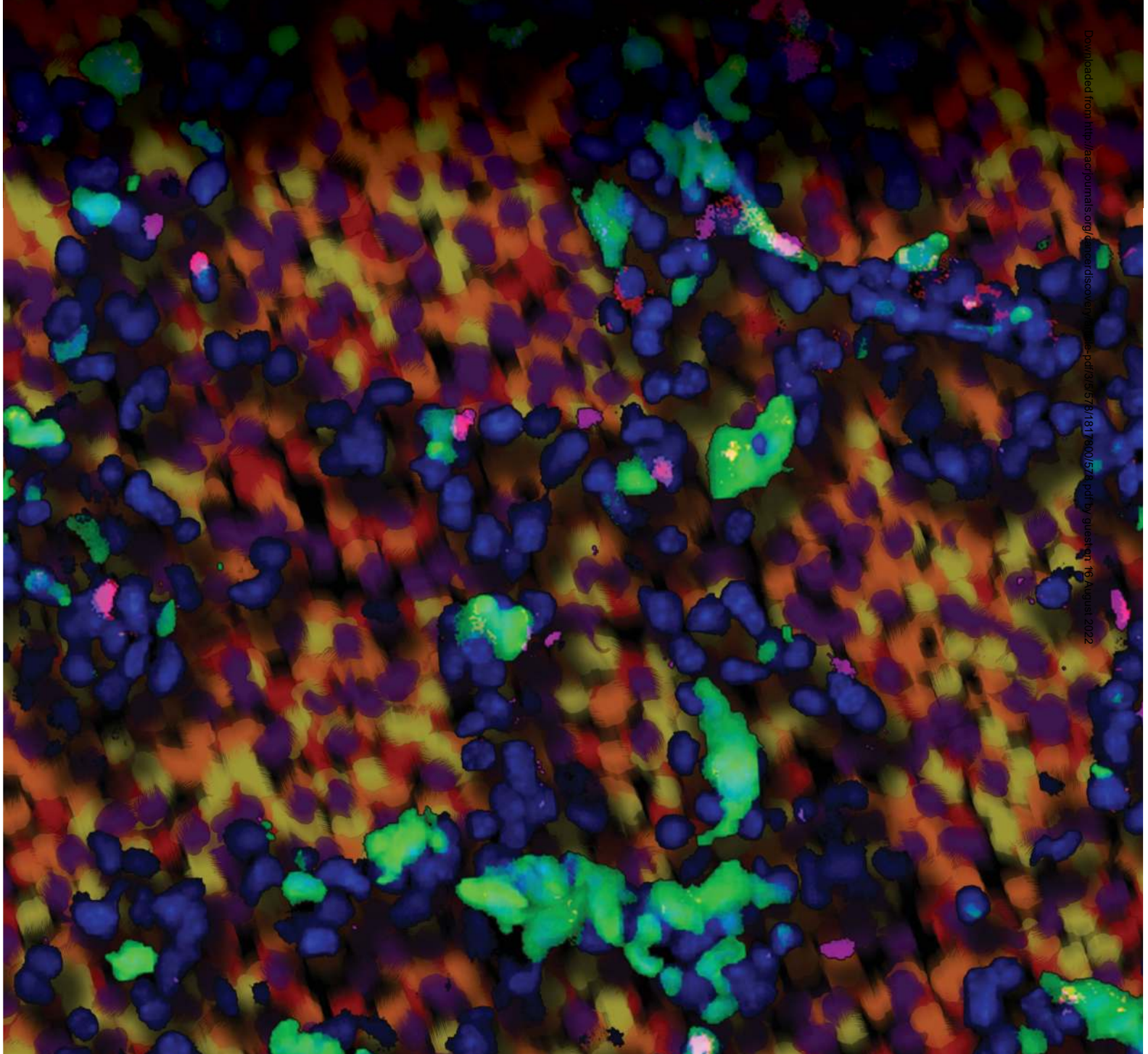

ABSTRACT Metastatic tumors have been shown to establish permissive microenvironments for metastases via recruitment of bone marrow–derived cells. Here, we show that metastasis-incompetent tumors are also capable of generating such microenvironments. However, in these situations, the otherwise prometastatic Gr1$^+$ myeloid cells create a metastasis-refractory microenvironment via the induction of thrombospondin-1 (Tsp-1) by tumor-secreted prosaposin. Bone marrow–specific genetic deletion of Tsp-1 abolished the inhibition of metastasis, which was restored by bone marrow transplant from Tsp-1$^+$ donors. We also developed a 5-amino acid peptide from prosaposin as a pharmacologic inducer of Tsp-1 in Gr1$^+$ bone marrow cells, which dramatically suppressed metastasis. These results provide mechanistic insights into why certain tumors are deficient in metastatic potential and implicate recruited Gr1$^+$ myeloid cells as the main source of Tsp-1. The results underscore the plasticity of Gr1$^+$ cells, which, depending on the context, promote or inhibit metastasis, and suggest that the peptide could be a potential therapeutic agent against metastatic cancer.

SIGNIFICANCE: The mechanisms of metastasis suppression are poorly understood. Here, we have identified a novel mechanism whereby metastasis-incompetent tumors generate metastasis-suppressive microenvironments in distant organs by inducing Tsp-1 expression in the bone marrow–derived Gr1$^+$ myeloid cells. A 5-amino acid peptide with Tsp-1–inducing activity was identified as a therapeutic agent against metastatic cancer. *Cancer Discov; 3(5); 578–89. ©2013 AACR.*

INTRODUCTION

The vast majority of cancer-related deaths are caused by organ failure brought about by metastatic dissemination of tumor cells. At the metastatic site, the disseminated tumor cells proliferate and induce angiogenesis to allow further tumor outgrowth to form lethal macrometastases (1–3). However, despite our increased understanding of the physiologic processes involved in tumor metastasis, no clinically approved drugs have shown significant efficacy at treating advanced, metastatic cancer. As early as 1889, Stephen Paget set forth his "seed" and "soil" hypothesis establishing the concept that breast cancer metastasizes to specific organs that harbor a receptive microenvironment (4). Experimental support for this hypothesis has been provided by the demonstration that primary tumors release specific cytokines, such as VEGF, stromal cell–derived factor 1 (SDF-1), TGF-β, and TNF-α, which systemically initiate premetastatic niches, characterized by the accumulation of bone marrow–derived cells such as VEGF receptor (VEGFR)1$^+$ hematopoietic cells and CD11b$^+$ myeloid cells (5). Furthermore, these premetastatic niches are characterized by the selective induction of organ-specific chemoattractants, growth factors, and extracellular matrix–related proteins, including fibronectin, lysyl oxidase, and S100A8 (6–9). Although these studies have provided key insights into metastasis-promoting niches, the existence of niches that may confer metastasis suppression, has not been examined.

In this study, we show that tumors that are deficient in metastatic potential are as capable of recruiting bone marrow–derived myeloid cells to potential metastatic organs as highly metastatic tumors. However, metastasis-incompetent tumors systemically stimulate expression of the antitumorigenic factor Tsp-1 in the recruited CD11b$^+$Gr1$^+$ cells, converting these prometastatic cells into metastasis-inhibitory cells that are refractory to the outgrowth of metastatic tumor cells. As such, our study provides a novel insight into the exquisite functional plasticity of the Gr1$^+$ cells previously shown to enhance carcinogenesis (10–12). Moreover, we describe the development of a novel peptide that stimulates Tsp-1 in Gr1$^+$ cells and blunts metastasis when administered systemically.

RESULTS

Poorly Metastatic Tumors Recruit Bone Marrow–Derived Cells to the Premetastatic Microenvironment in the Lungs

It has been shown that metastatic tumors are able to induce the recruitment of bone marrow–derived cells to future sites of metastasis, creating a permissive microenvironment for colonization (5). However, no analysis has determined whether this process is impaired in metastasis-incompetent tumors or if

Authors' Affiliations: Departments of [1]Cardiothoracic Surgery and [2]Cell and Developmental Biology, [3]Neuberger Berman Lung Cancer Center, Weill Cornell Medical College of Cornell University, New York, New York; [4]Vascular Biology Program, Boston Children's Hospital; [5]Department of Surgery, Harvard Medical School, Boston, MA; and [6]The Gade Institute, Section for Pathology, University of Bergen and [7]Department of Urology, Haukeland University Hospital, Bergen, Norway

Note: Supplementary data for this article are available at Cancer Discovery Online (http://cancerdiscovery.aacrjournals.org/).

N. Bhattacharya and T. El Rayes contributed equally to this work.

Corresponding Authors: Vivek Mittal, Departments of Cardiothoracic Surgery and Cell and Developmental Biology, Neuberger Berman Lung Cancer Center, Weill Cornell Medical College of Cornell University, 1300 York Avenue, 525 East 68th Street, New York 10065, NY. Phone: 212-746-9401; Fax: 212-746-9393; E-mail: vim2010@med.cornell.edu; and Randolph S. Watnick, Vascular Biology Program, Department of Surgery, Boston Children's Hospital, Harvard Medical School, Karp Family Research Laboratories, 11:212, 300 Longwood Avenue, Boston, MA 02115. Phone: 617-919-2427; E-mail: Randy.Watnick@childrens.harvard.edu

doi: 10.1158/2159-8290.CD-12-0476

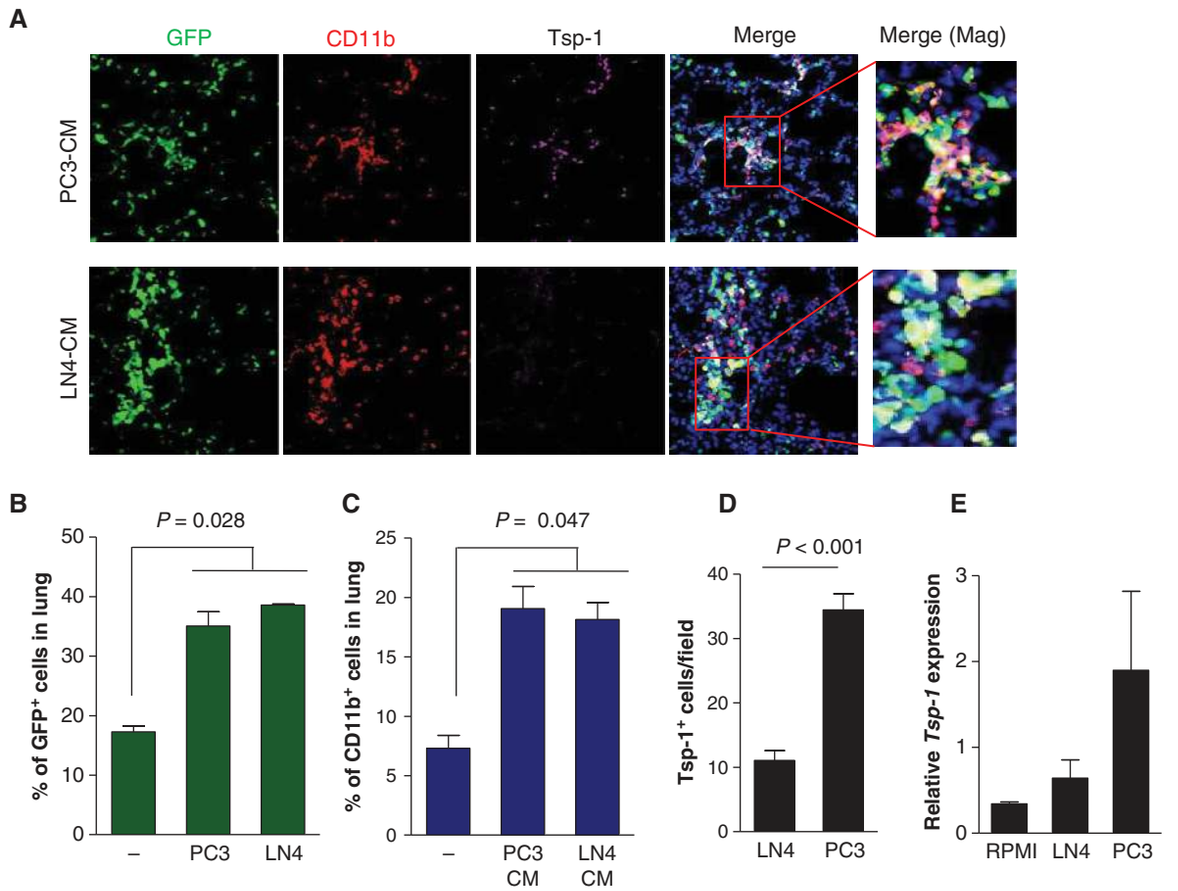

Figure 1. Conditioned media (CM) from metastasis-incompetent tumor cells induce Tsp-1 in the lung microenvironment. **A,** representative immunofluorescence images showing recruitment of GFP$^+$ bone marrow–derived cells in the lungs of mice treated with PC3 CM compared with LN4 CM. Elevated Tsp-1 expression is observed in a population of CD11b$^+$ cells in the lungs of mice treated with PC3 CM. 4′, 6-diamidino-2-phenylindole (DAPI) was used to label the nuclei of cells. Magnified images on the right show colocalization of signals. **B,** flow cytometry–based quantitation of recruited bone marrow–derived GFP$^+$ cells in lungs of mice treated with control serum-free RPMI media (–), LN4 CM, or PC3 CM ($n = 3$ per group). **C,** flow cytometry–based quantitation of recruited CD11b$^+$ cells in lungs of mice treated with control serum-free RPMI media (–), LN4 CM, or PC3 CM. ($n = 3$ per group). **D,** quantitation of CD11b$^+$ cells expressing Tsp-1 in the lungs after 1-week challenge with PC3 CM or LN4 CM. ($n = 16$, 4 random fields from 4 mice per group, $P < 0.001$). **E,** quantitative real-time PCR analysis of *Tsp-1* expression in lungs of control RPMI, PC3, or LN4 CM-treated mice ($n = 3$ mice).

these tumors create metastasis-refractory microenvironments. To determine whether tumors that lack robust metastatic capabilities are able to generate metastasis-suppressive niches in distant organs, we examined human prostate and breast cancer models that exhibit varying grades of metastatic potential (13, 14). These included weakly metastatic parental cells, PC3 or MDA-MB-231, and their highly metastatic variants, PC3M-LN4 (LN4) and MDA-MB-LM2 (LM2), respectively. To mimic the paracrine and endocrine effects of tumor-secreted factors on the premetastatic niche in the lung microenvironment *in vivo*, we administered conditioned media (CM) prepared from either the prostate or breast cancer cells to mice. To visualize the bone marrow–derived metastatic microenvironment, we conducted bone marrow transplantation (BMT) of wild-type (WT) mice with syngeneic *GFP*$^+$ bone marrow (2, 15). The CM from metastatic LN4 cells was able to efficiently increase the recruitment and formation of a GFP$^+$ bone marrow–derived premetastatic microenvironment, as would have been predicted (Fig. 1A and B). Strikingly, the CM from weakly metastatic PC3 tumor cells was also able to generate these microenvironments with similar efficiency (Fig. 1A and B). Further analysis revealed that the GFP$^+$ bone marrow cells recruited in both cases were predominantly CD11b$^+$ myeloid cells (Fig. 1A–C, Supplementary Figs. S1A and S1B).

Poorly Metastatic Tumors Induce Tsp-1 Expression in the Bone Marrow–Derived Cells in the Premetastatic Microenvironment

Having observed no differences in the cellular composition of premetastatic lungs generated by metastasis-competent and incompetent tumors, we postulated that the bone marrow–derived cells recruited by the different tumor types might exhibit molecular differences that would provide insights into metastasis-resistant microenvironments. As such, we conducted gene expression analysis of lungs of PC3 and LN4 CM-treated mice (Supplementary Fig. S2). Among the genes differentially regulated by PC3 CM, we focused on those encoding secreted proteins that are most likely to reprogram the local microenvironment and exert a negative impact on metastatic outgrowth of tumor cells. Among candidate genes, thrombospondin-1 (*Tsp-1*) was selected for further analysis, as it encodes a secreted

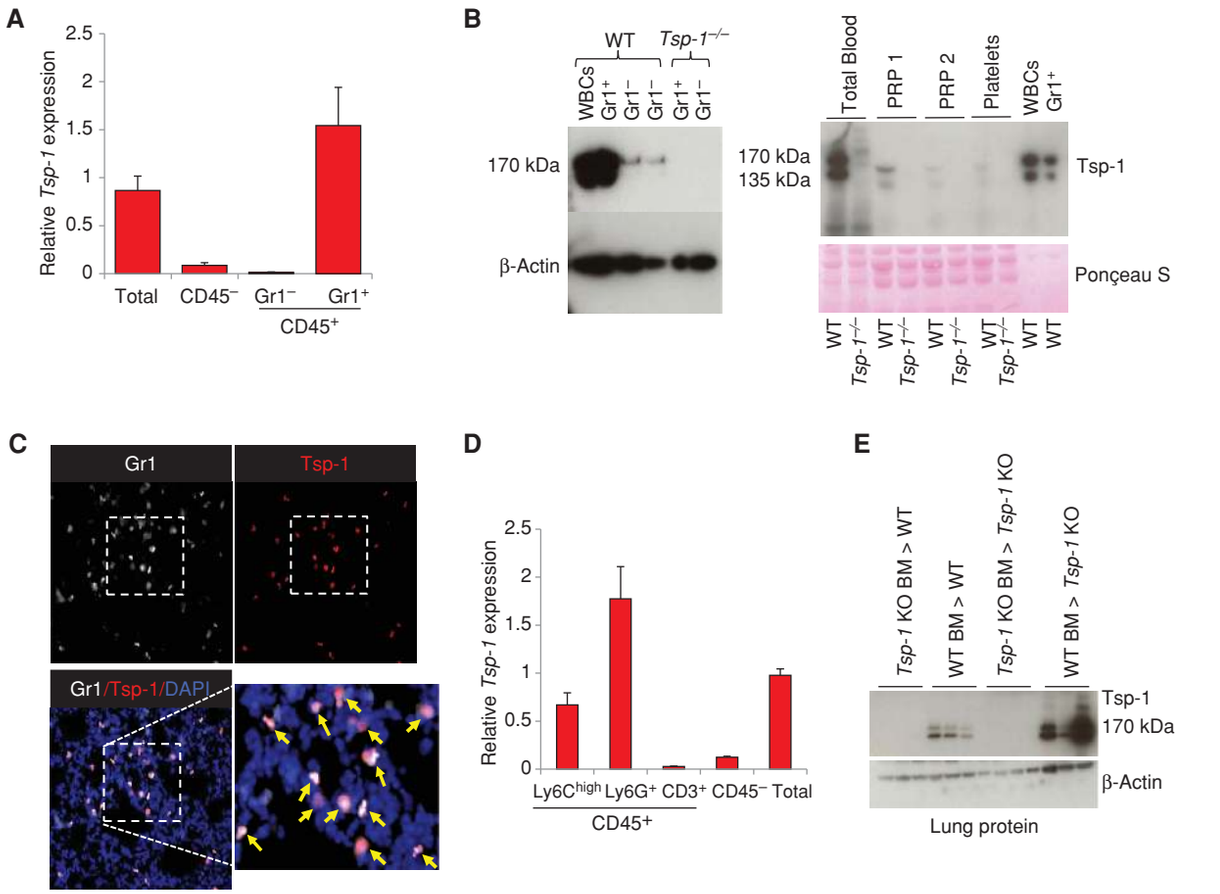

Figure 2. *Tsp-1* expression is mainly confined to bone marrow–derived Gr1$^+$ cells. **A,** quantitative RT-PCR analysis of *Tsp-1* expression in different subsets of flow sorted CD45$^+$ bone marrow hematopoietic cells isolated from the lung. Of these, the Gr1$^+$ cells showed elevated Tsp-1 compared with Gr1$^-$ cells or other CD45$^-$ cells. Total lung, all cells from the lung. **B,** Western blot analysis of Tsp-1 levels in cellular hematopoietic compartments in the peripheral blood from WT mice and *Tsp-1*$^{-/-}$ mice show Gr1$^+$ cells as a major source of Tsp-1. WBC, white blood cells; PRP, platelet-rich plasma. **C,** immunofluorescence staining of lungs showing expression of Tsp-1 by Gr1$^+$ cells. The boxed area highlights Tsp-1–expressing Gr1$^+$ cells depicted by arrows. **D,** quantitative RT-PCR analysis of Tsp-1 expression in different subsets of sorted bone marrow (BM)-hematopoietic cells from the lung. Both subsets of Gr1$^+$ cells, Ly6C^{high}, and Ly6G$^+$ cells express *Tsp-1*. **E,** Western blot analysis of Tsp-1 levels in lungs of mice after bone marrow transplantation. Transplantation of *Tsp-1*$^{-/-}$ bone marrow (BM) to WT recipients [*Tsp-1* knockout (KO) BM > WT] rendered lungs devoid of Tsp-1. Conversely, transplantation of WT BM to *Tsp-1*$^{-/-}$ recipients (WT BM > *Tsp-1* KO) restored Tsp-1 expression in the lung. WT BM > WT: transplantation of WT BM into WT recipients. *Tsp-1* KO BM > Tsp1 KO: transplantation of *Tsp-1*$^{-/-}$ BM into *Tsp-1*$^{-/-}$ recipients.

extracellular matrix protein and one of the most potent inhibitors of tumor angiogenesis and growth (16, 17). Both cell count and real-time (RT)-PCR analysis confirmed that Tsp-1 was upregulated in the lungs of PC3 CM-treated mice compared with controls or LN4 CM-treated mice (Fig. 1D and E).

Bone Marrow–Derived CD11b$^+$Gr1$^+$ Myeloid Cells Are the Major Contributors of Tsp-1

We next conducted an immunostaining analysis to determine the source of Tsp-1 in the lung stroma and observed that Tsp-1 expression was mainly confined to the bone marrow–derived CD11b$^+$ cells recruited in the lungs of mice treated with PC3 CM (Fig. 1A, Supplementary Fig. S1A). Conversely, we observed no discernible induction of Tsp-1 expression in the lungs of mice treated with LN4 CM (Fig. 1A). To further assess which bone marrow cell populations expressed Tsp-1, we analyzed specific flow-sorted bone marrow cell populations from the lungs by RT-PCR (Fig. 2A) and observed that Tsp-1 expression was largely confined to Gr1$^+$ myeloid cells and not the Gr1$^-$ myelocytes or other hematopoietic cells (Fig. 2A). To further exclude the possibility that other cell types might also express Tsp-1, we conducted a Western blot analysis of different cellular components from peripheral blood harvested from WT mice or *Tsp-1* knockout (KO) (*Tsp-1*$^{-/-}$) mice. Notably, the Gr1$^+$ cells expressed abundant Tsp-1 compared with Gr1$^-$ cells (Fig. 2B ; Supplementary Fig. S3A). As expected, there was a complete lack of Tsp-1 in all compartments examined in *Tsp-1*$^{-/-}$ mice (Fig. 2B).

Further analysis of the peripheral blood showed that Gr1$^+$ cells express predominantly the higher-molecular-weight isoforms of Tsp-1 (160–170 kDa), whereas the platelets express a lower-molecular-weight isoform (135–140 kDa; Fig. 2B, right). Indeed, both forms have been observed previously in platelets (18). Importantly, Gr1$^+$ cells expressed higher levels of Tsp-1 compared with the platelets. Taken together, these data indicate that the bone marrow–derived Gr1$^+$ cells are

the major source of Tsp-1 in the premetastatic microenvironments generated by weakly metastatic tumors.

Given that immunostaining analysis confirmed that Tsp-1 expression was confined to $Gr1^+$ cells (Fig. 2C) and the $Gr1^+$ population is composed of 2 major subpopulations; $Ly6G^+$ granulocytic myeloid cells and $Ly6C^{high}$ myelomonocytic cells, we further analyzed these $Gr1^+$ subpopulations (Supplementary Fig. S3B). Our analyses revealed that both subsets of $Gr1^+$ cells expressed Tsp-1 (Fig. 2D). To conclusively determine that the chief source of Tsp-1 expression in the lungs was the $Gr1^+$ bone marrow cells and not other lung stromal cells, we conducted BMT experiments. We observed Tsp-1 expression in the lungs of *Tsp-1*$^{-/-}$ mice that were transplanted with WT bone marrow but not in WT mice transplanted with *Tsp-1*$^{-/-}$ bone marrow (Fig. 2E).

To exclude the possibility that these findings were somehow unique to the prostate cancer model, we examined a breast cancer model as well. As described above, we used the weakly metastatic parental cells, MDA-MB-231 (MDA), and their highly metastatic variants, MDA-MB-LM2 (LM2). Consistent with the observations in the prostate cancer model, CM from weakly metastatic MDA breast cancer cells also induced upregulation of Tsp-1 expression in bone marrow-recruited $Gr1^+$ cells as compared with CM from highly metastatic LM2 breast cancer cells (Supplementary Fig. S4). These results, when taken together, strongly indicate that bone marrow–derived cells are the exclusive source of Tsp-1 induced by weakly metastatic tumors in the lungs.

Genetic Deletion of *Tsp-1* in the Bone Marrow Results in Increased Metastasis

We next postulated that expression of Tsp-1 in recruited $Gr1^+$ myeloid cells in the lungs could generate a metastasis-refractory environment. To test the significance of bone marrow–derived Tsp-1 in modulating metastasis, we generated Tsp-1 deficiency in the bone marrow. Specifically, we harvested bone marrow cells from *Tsp-1*$^{-/-}$ mice and transplanted these cells into irradiated syngeneic WT mice to generate a cohort of *Tsp-1*$^{-/-}$ BMT mice. As controls, bone marrow from WT mice was transplanted into irradiated WT mice to generate a cohort of WT BMT control mice. As expected of a successful BMT and engraftment of recipient mice with donor bone marrow, Western blot and RT-PCR analysis of peripheral blood leukocytes from *Tsp-1*$^{-/-}$ BMT mice showed undetectable Tsp-1 protein levels and low mRNA levels compared with WT BMT controls (Supplementary Figs. S5A and S5B).

We then sought to determine the impact on metastasis of bone marrow–derived Tsp-1 in the lung microenvironment. As such, we examined the ability of Lewis lung carcinoma cells (LLC) to colonize the lungs of mice that received a bone marrow transfer from WT mice or *Tsp-1*$^{-/-}$ mice. Specifically, we injected LLC cells stably expressing the firefly luciferase gene (LLC-luc) (2, 14) via tail vein and monitored lung metastases. Strikingly, we observed accelerated metastases in *Tsp-1*$^{-/-}$ BMT mice compared with WT BMT mice (Fig. 3A and B). Western blot analysis of the total lung lysates showed complete absence of Tsp-1 in the lungs of *Tsp-1*$^{-/-}$ BMT mice (Fig. 3C), indicating that in a metastatic setting the bone marrow–derived cells are the main source of Tsp-1 in the lung parenchyma. Moreover, as expected, in *Tsp-1*$^{-/-}$ BMT mice, the $Gr1^+$ cells were devoid of Tsp-1 expression (Supplementary Fig. S6). Importantly, Tsp-1 deficiency in the bone marrow cells in *Tsp-1*$^{-/-}$ BMT mice did not perturb the recruitment of $Gr1^+$ cells in the lung microenvironment compared with WT BMT mice (Supplementary Fig. S6), nor did the lack of Tsp-1 perturb the biogenesis of other bone marrow hematopoietic cells (Supplementary Fig. S5C). To exclude the possibility that enhanced metastasis was due to differential tumor cell seeding in the lung parenchyma of *Tsp-1*$^{-/-}$ BMT mice, we conducted a seeding experiment. We found, via a time course evaluation of the lungs following administration of tumor cells, that seeding efficiency was comparable in the lungs of BMT mice regardless of the donor source (Supplementary Fig. S7).

To provide further evidence that the observed antimetastatic effect is due to Tsp-1 production in $Gr1^+$ cells, we conducted a reverse BMT experiment. Specifically, we transplanted bone marrow from WT mice into *Tsp-1*$^{-/-}$ mice. As a control, we transplanted bone marrow from *Tsp-1*$^{-/-}$ donors into *Tsp-1*$^{-/-}$ mice to account for any possible effects of the transplantation procedure. Strikingly, transplantation of WT bone marrow into *Tsp-1*$^{-/-}$ mice resulted in complete suppression of metastasis (Fig. 3D and E). This phenomenon was most likely due to the dramatically increased expression of Tsp-1 in the lungs of these mice compared with WT mice transplanted with WT bone marrow (Fig. 3F; Supplementary Fig. S8). Consistent with previous observations, Tsp-1 expression was restored in the $Gr1^+$ cells in *Tsp-1*$^{-/-}$ mice transplanted with WT bone marrow (Supplementary Fig. S8). These findings, support the hypothesis that supraphysiologic induction of Tsp-1 in $Gr1^+$ cells can blunt metastasis as well as the possibility that a therapeutic agent with such activity could be effective at treating advanced metastatic cancer.

Bone Marrow–Derived Tsp-1 Inhibits Metastatic Outgrowth through Inhibition of Tumor Cell Proliferation

The antitumor activity of Tsp-1 has been shown to be involved in tumor growth blockade through diverse mechanisms: angiogenesis inhibition, blockade of cell proliferation, and induction of apoptosis both in tumor cells and endothelial cells (19, 20). Consistent with these functions, the metastatic lesions in the lungs of *Tsp-1*$^{-/-}$ BMT mice showed elevated proliferation of tumor cells compared with control WT BMT mice ($P = 0.002$; Fig. 3G, Supplementary Fig. S9), whereas the tumor cell apoptotic index remained unperturbed in the lungs of *Tsp-1*$^{-/-}$ BMT mice compared with control WT BMT mice, ($P = 0.09$, Fig. 3H). Taken together, these results show that Tsp-1 in recruited bone marrow–derived $Gr1^+$ cells did not affect metastatic seeding of tumor cells or their ability to stimulate angiogenesis, but impaired tumor outgrowth at the metastatic site by inhibiting tumor cell proliferation.

Stimulation of Tsp-1 in the Lung Microenvironment as a Potential Antimetastatic Approach

We next speculated about whether administration of Tsp-1 would constitute a potential antimetastatic strategy, as it has been postulated that Tsp-1 could be a potent clinical inhibitor of tumor progression and metastasis (16, 21, 22). However, the translational relevance of this approach has been

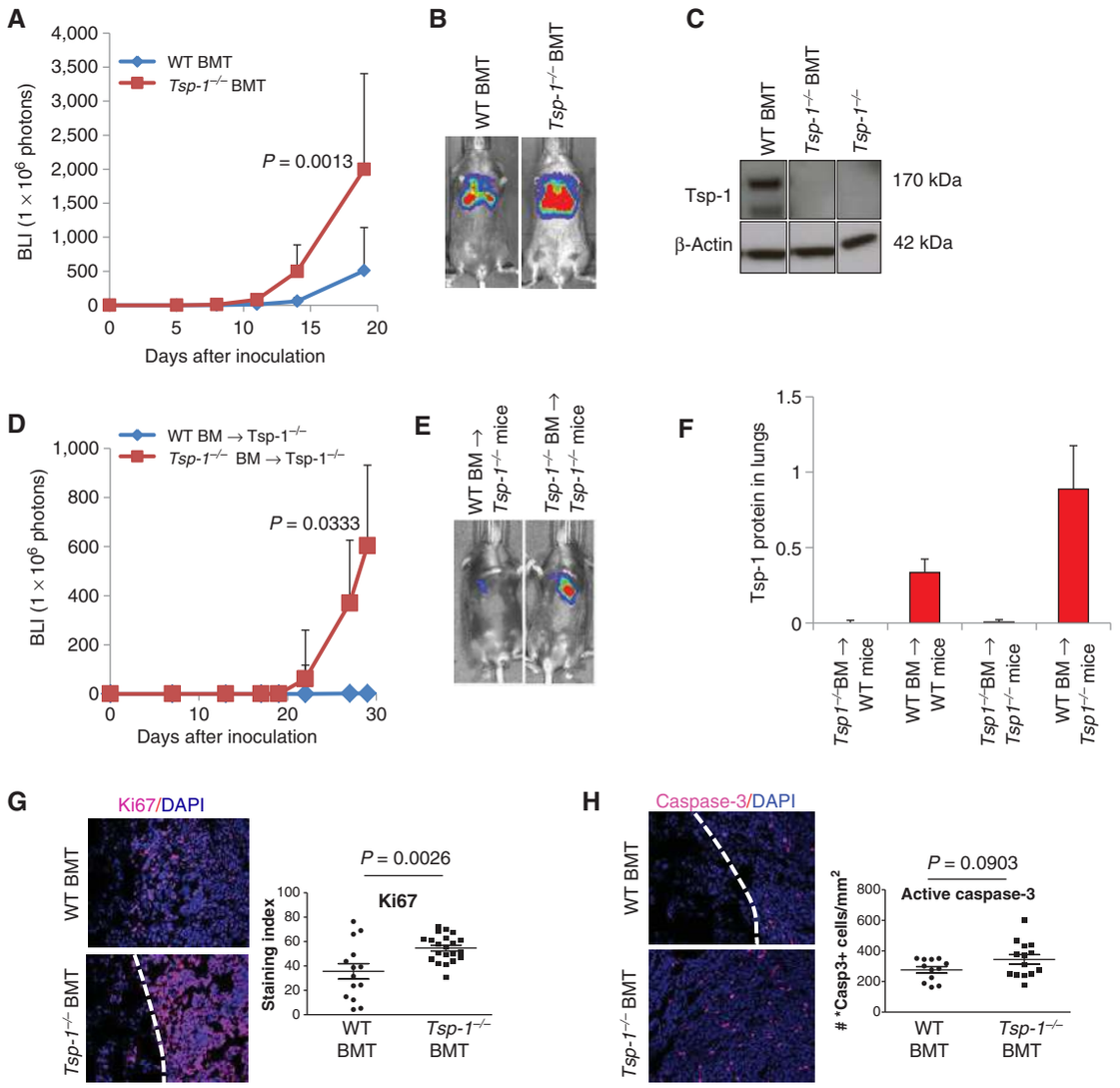

Figure 3. Bone marrow–derived Gr1$^+$ cells confer a metastasis-suppressive phenotype through the secretion of Tsp-1. **A,** quantitation of pulmonary metastases in WT BMT mice and *Tsp-1*$^{-/-}$ BMT mice ($n = 7$ per group). BLI estimates were obtained at days 0, 5, 8, 11, 14, and 19 following tail vein injections of 1×10^5 LLC cells. $P = 0.0013$ between WT BMT and Tsp-1$^{-/-}$ BMT groups at day 19. **B,** representative BLI images showing metastasis suppression in WT BMT mice compared with *Tsp-1*$^{-/-}$ BMT mice depicted in **A**. **C,** Western blot analysis of Tsp-1 from the lungs of WT BMT mice and *Tsp-1*$^{-/-}$ BMT mice. Lung from whole-body *Tsp-1*$^{-/-}$ mice was used as a control. **D,** quantitation of pulmonary metastases in *Tsp-1*$^{-/-}$ mice transplanted with WT bone marrow and Tsp-1$^{-/-}$ mice transplanted with Tsp-1$^{-/-}$ bone marrow ($n = 5$ per group). BLI estimates were obtained following tail vein injections of 1×10^5 LLC cells. $P = 0.033$ between the 2 groups at day 30. **E,** representative BLI images showing metastasis suppression in *Tsp-1*$^{-/-}$ mice transplanted with WT bone marrow compared with *Tsp-1*$^{-/-}$ mice transplanted with *Tsp-1*$^{-/-}$ bone marrow depicted in **D**. **F,** quantitation of Tsp-1 protein expression in the lungs of mice following BMT. **G,** left, representative immunofluorescence images showing Ki67$^+$ cells in the metastatic lungs of WT BMT mice and *Tsp-1*$^{-/-}$ BMT mice. Right, quantitation of Ki67$^+$ cells. Sections were evaluated from 6 animals per group. **H,** left, representative immunofluorescence images showing active caspase-3$^+$ cells in the metastatic lungs of WT BMT mice and Tsp-1$^{-/-}$ BMT ($P = 0.0903$). Right, quantitation of active caspase-3$^+$ cells. Sections were evaluated from 6 animals per group. White dotted line in **G** and **H** is the demarcation of the tumor/normal tissue.

minimized by the fact that Tsp-1 is an extremely large protein that is not feasible to use as a therapeutic agent (23). Indeed, a mimetic nonapeptide derived from the type I repeat of Tsp-1, which contains the antiangiogenic activity of the endogenous protein, has been developed. However, in clinical trials, this drug showed little efficacy due, in part, to its inability to fully replicate the activity of the full-length protein (24, 25). We reasoned that to effectively use Tsp-1 as a therapeutic agent, it would be necessary to induce the expression of full-length Tsp-1, containing all of its inhibitory activity, in the premetastatic lung, particularly in the bone marrow cells. We therefore turned our attention to prosaposin (Psap), a precursor of sphingolipid activator proteins, which was previously shown to stimulate the expression of Tsp-1 in human lung fibroblasts *in vitro* (14). Indeed, breast cancer CM from MDA cells stimulated Tsp-1 in the Gr1$^+$ cells in the lungs, as expected. However, CM from MDA cells expressing *Psap*-short hairpin RNA (shRNA) failed to induce Tsp-1 expression in the Gr1$^+$

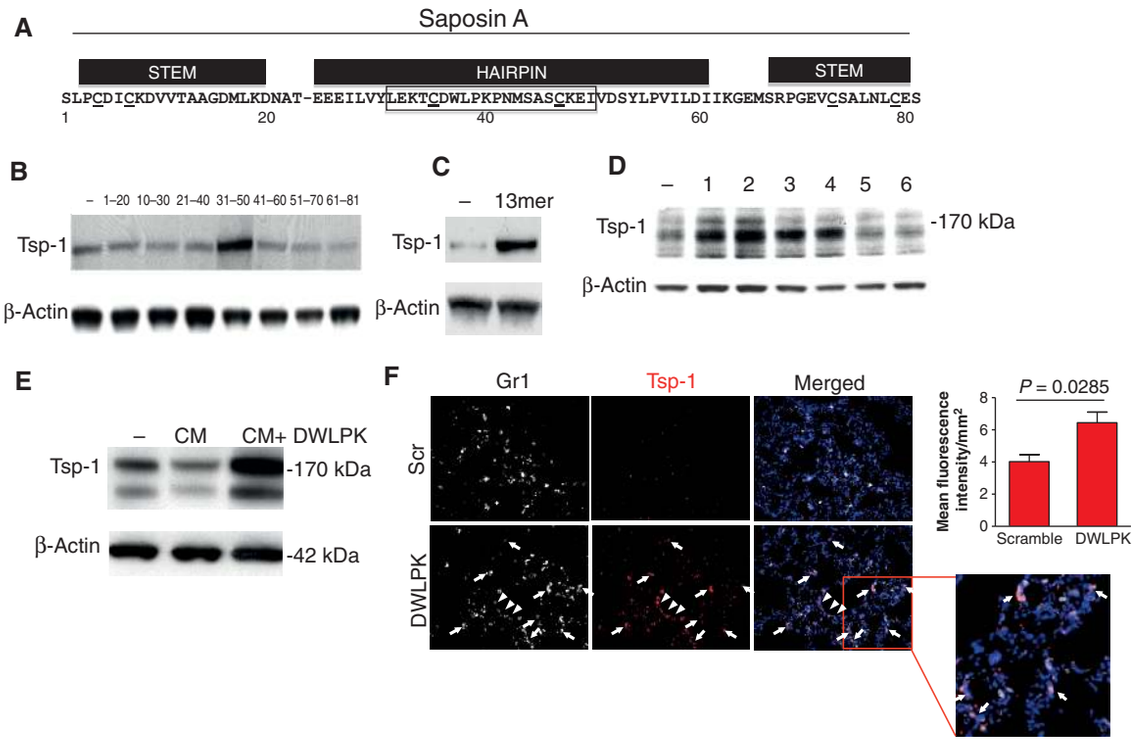

Figure 4. Development of a Psap-mimetic peptide as a pharmacologic approach to upregulate Tsp-1 expression in the lungs. **A,** amino acid sequence of human saposin A. The stem and hairpin regions are depicted above the sequence. The 6 conserved cysteines are underlined. The boxed region represents the 20-amino acid peptide spanning residues 31–50 of saposin A, capable of stimulating the expression of Tsp-1. **B,** Western blot analysis of Tsp-1 expression in WI-38 fibroblasts treated with 7 overlapping 20-amino acid peptides (1–20, 10–30, 21–40, 31–50, 41–60, 51–70, and 61–81) spanning the length of saposin A. **C,** Western blot analysis of Tsp-1 in WI-38 fibroblasts that were untreated (–) or treated with a cyclic 13-amino acid peptide corresponding to residues 35–47 of saposin A. **D,** Western blot analysis of Tsp-1 expression in WI-38 fibroblasts that were untreated (–) or treated with 6 peptides derived from amino acids 35–40 of saposin A ranging from 3–6 amino acids in length (1 = CDWLPK, 2 = CDWLP, 3 = DLWPK, 4 = DWLP, 5 = CDW, 6 = DWL). **E,** Western blot showing Tsp-1 levels in mouse lung tissue following administration of media alone (–), LN4 CM (CM), or LN4 CM with 30 mg/kg/d Psap peptide (DWLPK). **F,** representative immunofluorescence images of lungs showing Tsp-1 expression by Gr1$^+$ cells in mice treated with DWLPK compared with a scrambled peptide (Scr). Representative images were generated from lungs of 3 mice per group (4 sections per mouse, 7–12 fields per section). Arrows indicate colocalization of Gr1 and Tsp-1. Right, quantitation showing Tsp-1 levels in the lungs of mice treated with either Scr or DWLPK peptide shown in the left. Identical results obtained in multiple repeat experiments.

cells (Supplementary Fig. S10A and S10B). We also examined the prostate cancer model, and as expected, Western blot analysis showed elevated Tsp-1 levels in the lungs of PC3 CM-treated mice compared with LN4 CM treatment (Supplementary Fig. S10C). However, CM from isogenic PC3 cells in which *Psap* expression was silenced by shRNA (PC3-sh*Psap*) failed to enhance Tsp-1 levels in the lungs (Supplementary Fig. S10C).

We also examined whether overexpression of Psap in metastatic prostate cells from the orthotopic site would stimulate Tsp-1 in the lungs. Orthotopic prostate tumors were generated by injecting either metastatic LN4 cells or LN4 cells overexpressing Psap (LN4-Psap) in the prostate gland of mice. As expected, LN4-Psap tumors induced robust Tsp-1 expression in the premetastatic lungs compared with LN4 tumors (Supplementary Fig. S10D). Taken together, these results suggest that nonmetastatic tumor cells, by virtue of expressing Psap, systemically elevate Tsp-1 in the recruited bone marrow–derived Gr1$^+$ cells in an endocrine fashion.

We next postulated that Psap might directly enhance the expression of Tsp-1 in recruited Gr1$^+$ myeloid cells in the lungs to generate a metastasis-refractory environment. To determine whether the ability of Psap to inhibit metastasis via stimulation of Tsp-1 could be translated into a smaller, more easily deliverable agent, we sought to determine the minimal active region of the Psap protein. We first generated *Psap* truncation mutants, which contain saposin A, saposin AB, saposin ABC, and saposin BCD (Supplementary Fig. S11A) and ectopically expressed these mutants in LN4 cells. We then analyzed CM from these cells to determine which version harbored Tsp-1–stimulating activity. All truncation mutants except saposin BCD were able to stimulate Tsp-1 activity to the same level as the full-length protein (Supplementary Fig. S11A). Thus, we concluded that saposin A contains the Tsp-1–stimulating activity of Psap. We next sought to determine whether there was a smaller domain within saposin A that contained the Tsp-1–stimulating activity. Accordingly, we generated seven 20-amino acid overlapping peptides spanning the 81-amino acid sequence of saposin A (Fig. 4A). We observed that a 20-amino acid peptide spanning residues 31–50 of saposin A was the only peptide capable of stimulating the expression of Tsp-1 (Fig. 4B). We then examined the crystal structure of saposin A and determined that residues 31–50 reside in the hairpin region between helices 2 and 3 (Supplementary Fig. S11B; ref. 26). Accordingly, we tested a cyclic 13-amino acid peptide, corresponding to residues 35–47, constrained by a disulfide bond between cysteine residues at each end of the

peptide. The cyclic peptide was able to stimulate Tsp-1 (Fig. 4C). We then tested a 6-amino acid peptide, CDWLPK, corresponding to the first 6 residues of the cyclic peptide and found that it also was able to stimulate Tsp-1 (Fig. 4D). Finally, we tested 6 peptides from within the 6-amino acid sequence of CDWLPK. Of these peptides, we found that both a 5-amino acid peptide (DWLPK) and a 4-amino acid peptide (DWLP) were able to stimulate Tsp-1 expression to an even greater extent than CDWLPK (Fig. 4D). We then tested the 5-amino acid peptide in the *in vivo* assay by administering it to mice in combination with CM from LN4 cells and observed that it was able to stimulate Tsp-1 in the lungs of these mice (Fig. 4E).

Having determined that the 5-amino acid DWLPK peptide derived from Psap retains the Tsp-1–stimulating activity of the full-length Psap both *in vitro* and *in vivo*, we sought to determine whether it also targeted bone marrow–derived cells. As such, we treated mice with CM from LN4 cells alone to simulate a systemic tumor-induced recruitment of bone marrow–derived stromal cells in the lungs, or CM in combination with DWLPK peptide. As expected, the recruitment of $Gr1^+$ cells was identical regardless of the treatment (Supplementary Fig. S12A). However, administration of the DWLPK peptide stimulated Tsp-1 expression in the $Gr1^+$ cells by more than 2-fold, whereas a peptide composed of the same amino acids in a scrambled sequence failed to stimulate Tsp-1 (Fig. 4F, Supplementary Fig. 12B). The induction of Tsp-1 occurred systemically, as shown by Western blot analysis of peripheral leukocytes from peptide-treated mice (Supplementary Fig. 12C).

These results suggest that the Tsp-1–enhancing activity of Psap is confined to a 5-amino acid peptide and that administration of this peptide could create a Tsp-1–mediated metastasis-suppressive microenvironment.

Psap Mimetic Peptide (DWLPK) Inhibits Metastases through Stimulation of Tsp-1 in the $Gr1^+$ Cells

To determine whether Psap peptide-mediated stimulation of Tsp-1 by bone marrow $Gr1^+$ cells in the lung parenchyma confers a metastasis-resistant niche, we administered LLC-luc cells via tail vein into WT mice treated with either DWLPK peptide or scrambled control. Strikingly, administration of the DWLPK peptide dramatically reduced lung metastases compared with the scrambled peptide, as measured by bioluminescence imaging (BLI; Fig. 5A and B). Notably, metastatic lungs from mice (day 30) treated with DWLPK peptide showed persistent Tsp-1 upregulation in the $Gr1^+$ myeloid compartment compared with treatment with scrambled peptide (Fig. 5C, Supplementary Fig. S12B). In agreement with previous observations, immunostaining and RT-PCR analysis showed that the Tsp-1 expression was confined to the $Gr1^+$ cells and not to the $Gr1^-$ stromal cells, which included $F4/80^+$ macrophages (Fig. 5C, Supplementary Fig. S13).

To confirm that the DWLPK peptide-induced Tsp-1 expression in the bone marrow cells was directly responsible for the antimetastatic phenotype, we conducted genetic deletion of Tsp-1 in the bone marrow by generating *Tsp-1*$^{-/-}$ BMT mice and used WT BMT mice as controls. Strikingly, the DWLPK peptide failed to inhibit metastases in *Tsp-1*$^{-/-}$ BMT mice, whereas it potently inhibited lung metastases in WT BMT mice (Fig. 5D and E). Histologic examination of the lungs showed increased size of nodules ($P = 0.0317$), as well as a higher percentage of macrometastases (>1 mm of diameter) in Tsp-$1^{-/-}$ BMT mice compared with control WT BMT mice treated with the Psap peptide (Fig. 5F and H).

Finally, we sought to determine whether our observations with the experimental metastasis models could be recapitulated with tumors generated in the orthotopic site. As such, we tested the ability of the DWLPK peptide to inhibit metastasis in an orthotopic, clinically relevant model of breast cancer metastasis to the lung. Metastatic MDA-MB-LM2 breast cancer cells expressing luciferase were injected orthotopically in the mammary glands of severe combined immunodeficient (SCID) mice. After 3 weeks of growth (Fig. 6A), primary tumors were surgically resected; one cohort of mice was treated daily with DWLPK peptide and another cohort with a scrambled peptide. Lung metastases were assessed 3 weeks after the primary tumor removal (week 6 after primary tumor injection). In DWLPK-treated mice, the metastatic burden in the lungs was significantly reduced by 50% compared with scrambled peptide-treated mice (Fig. 6B). Consistent with the mechanism of action of the peptide, Tsp-1 levels were elevated after systemic DWLPK administration, as shown by Western blot and immunofluorescence in lung extracts of these mice (Fig. 6C and D). Taken together, these results indicate that the 5-amino acid DWLPK Psap peptide could have significant efficacy in treating metastatic cancer via induction of Tsp-1 in bone marrow–derived cells in the lung microenvironment.

DISCUSSION

In this study, we have shown that metastasis can be acutely affected by the tumor-induced systemic reprogramming of the bone marrow–derived cells in the lung microenvironment. Strikingly, we observed that the very same bone marrow–derived myeloid cells that have previously been shown to promote metastasis can also be induced to inhibit metastasis by the endocrine activity of metastasis-incompetent primary tumors.

Research in metastasis suppression has been generally focused on cancer cell autonomous properties, and suppressors of metastatic tumor outgrowth, such as *KISS1*, *MKK4*, *p38*, and *MKK7*, have been identified (27, 28). Here, we have identified a novel mechanism whereby primary tumors systemically modulate the microenvironment in distal target organs to inhibit metastasis (Fig. 7A). Significantly, we show that tumors that are deficient in metastatic potential are as capable of recruiting bone marrow–derived $CD11b^+Gr1^+$ hematopoietic cells to potential metastatic organs as highly metastatic tumors. However, metastasis-incompetent tumors systemically stimulate expression of the antitumorigenic factor Tsp-1 in the recruited bone marrow cells, converting these cells, which would otherwise serve to stimulate metastasis, into metastasis-inhibitory cells. The Tsp-1–expressing bone marrow–derived cells thus establish a microenvironment in the potential metastatic site that is refractory to the outgrowth of metastatic tumor cells. Of significant interest is the fact that metastasis suppression was abrogated in *Tsp-1* knockout BMT mice. The requirement of Tsp-1 expression in bone marrow–derived cells suggests a novel mechanism of action in which recruited bone marrow–derived $Gr1^+$ cells are the chief source of Tsp-1 in the metastatic lung. This is

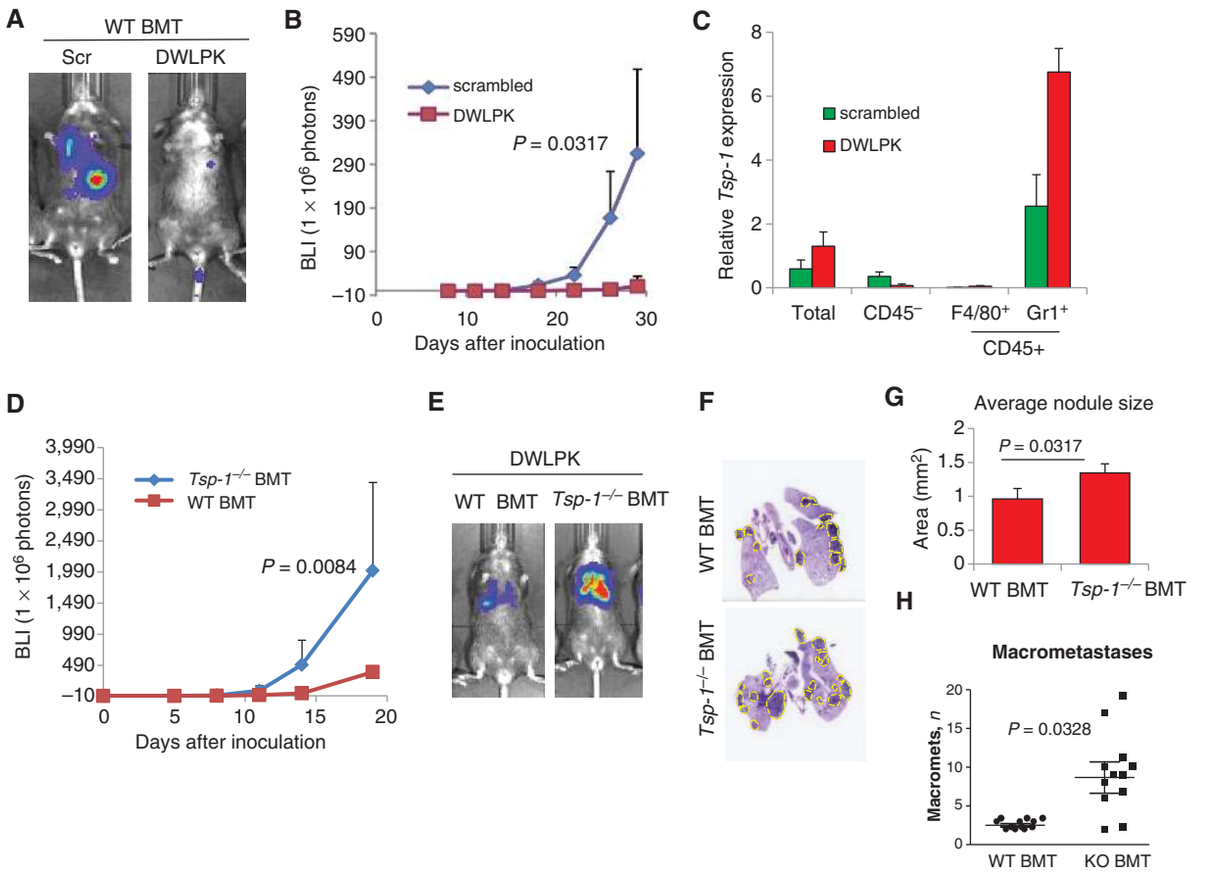

Figure 5. DWLPK peptide-mediated stimulation of Tsp-1 in the Gr1$^+$ cells results in suppression of lung metastases. **A,** representative BLI images of animals ($n = 5$ per group) showing suppression of lung metastases following tail vein injection of LLC cells in mice treated with DWLPK as compared with a scrambled peptide (Scr). Identical results were obtained in multiple repeat experiments. **B,** quantitation of pulmonary metastases by BLI. The BLI measurements were obtained at days 11, 14, 18, 22, 26, and 29 after inoculation of LLC cells. The relative BLI values show total photon count over time, $n = 10$. ($n = 5$ per group). $P = 0.0317$ between scrambled and DWLPK peptide-treated groups at day 29. Identical results were obtained in repeat experiments. **C,** quantitative RT-PCR showing *Tsp-1* levels in total lungs and flow cytometry–sorted CD45$^-$ cells and CD45$^+$ cells (F4/80$^+$ macrophages and Gr1$^+$ myeloid cells) from LLC metastases-bearing mice treated with DWLPK compared with scrambled peptide (scrambled; $n = 3$ per group). **D,** quantitation of pulmonary metastases in DWLPK peptide-treated WT BMT mice and *Tsp-1*$^{-/-}$ BMT mice ($n = 7$ per group). BLI estimates were obtained at days 0, 5, 8, 14, and 19 following tail vein injections of 1×10^5 LLC cells. *P* values between WT BMT and *Tsp-1*$^{-/-}$ BMT groups are $P = 0.0049$ and $P = 0.0084$ at days 14 and 19, respectively. **E,** representative BLI images showing DWLPK peptide-induced metastasis suppression in WT BMT mice compared with *Tsp-1*$^{-/-}$ BMT mice depicted in **D**. **F,** representative hematoxylin and eosin–stained lungs from mice in **E** showing metastases. **G,** quantitation of metastatic area in the lungs of WT BMT and *Tsp-1*$^{-/-}$ BMT mice ($n = 5$, each group). **H,** number of macrometastases (>1 mm diameter) in the lungs of WT BMT and *Tsp-1*$^{-/-}$ BMT mice ($n = 6$, each group).

consistent with published reports showing Tsp1 expression in monocyte/macrophage populations (29, 30).

Interestingly, we have previously shown that metastatic tumors induce metastasis-promoting potential in Gr1$^+$ cells recruited to the premetastatic lungs (31). However, depending on the nature of the tumor-derived systemic factor, the same cells can be modulated to exhibit metastasis-suppressive potential as shown in this study. It is thereby of great importance to decipher these pathways in the tumor milieu to further refine current therapies. Here, we show an example of an important antimetastatic effect of Gr1$^+$ cells.

Previously, we identified Psap as a tumor-secreted factor with antimetastatic activity. On the basis of these findings, a therapeutic strategy such as the 5-amino acid DWLPK peptide, which targets Gr1$^+$ bone marrow–derived cells in the microenvironment, could have significant efficacy in treating advanced metastatic cancer and ultimately in reducing the lethality of the disease.

From the perspective of targeting metastases, it has been emphasized that therapy should be targeted not only against tumor cells but also against the host microenvironment, which contributes to, and supports the progressive growth and survival of metastatic cancer cells (32). Given that the progression of human cancer to metastatic disease is the major contributing factor to its lethality, elevating Tsp-1 levels in the metastatic organ microenvironment to suppress metastasis may have clinical value. The Psap–Tsp-1 axis thus seems to be relevant *in vivo*. Significantly, examination of a tumor tissue microarray compiled from 103 patients with prostate cancer with long and complete follow-up revealed that Psap expression was positively correlated with increased overall survival. Specifically, patients with higher Psap levels in their primary

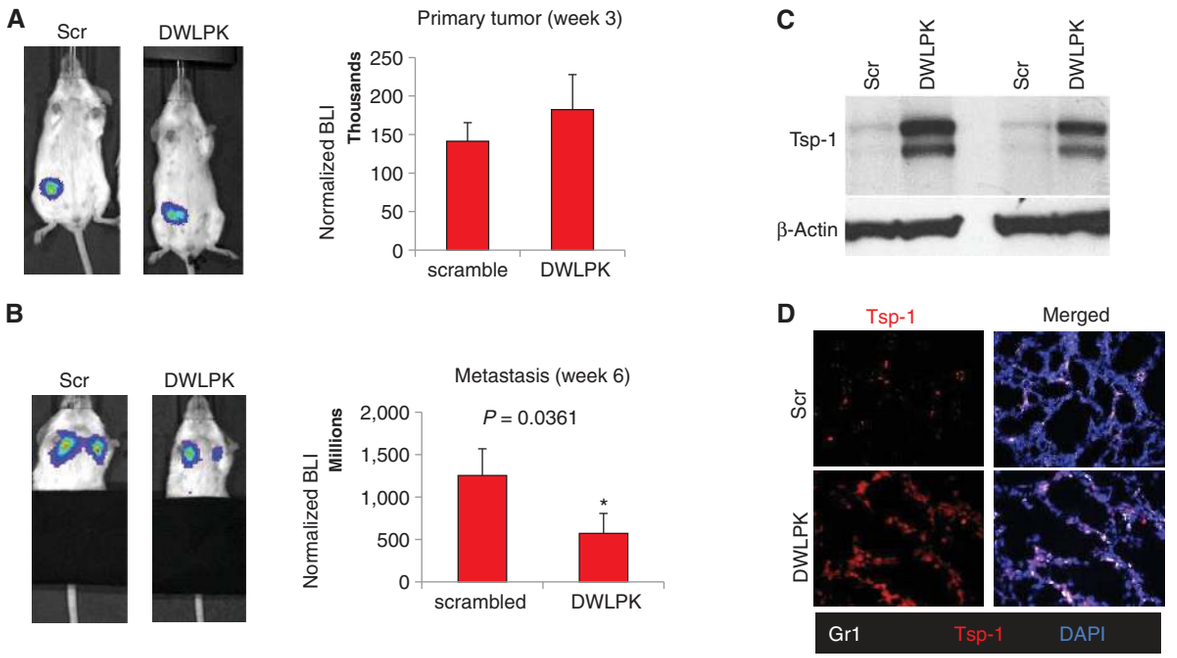

Figure 6. DWLPK peptide-mediated stimulation of Tsp-1 in the Gr1$^+$ cells results in suppression of lung metastases in an orthotopic breast cancer model. **A,** left, representative BLI images of animals showing orthotopic primary breast tumors derived from MDA-LM2 cells in the mammary gland of SCID mice (day 21). Right, quantitation of BLI reads from mice shown at left ($n = 6$). **B,** left, representative BLI images of lungs in mice from **A** treated with either a scrambled peptide or DWLPK peptide (images taken 3 weeks after surgical removal of primary tumors). Right, quantitation of BLI reads from mice shown at left ($n = 6$; $P = 0.037$, Mann–Whitney U test). **C,** Western blot analysis showing induction of Tsp-1 in the premetastatic lungs of LM2 tumor-bearing mice (3 weeks after primary tumor injection) treated with scrambled (Scr), or DWLPK peptide. Two representative mice per group shown; experiment was repeated and identical results obtained. **D,** representative images of premetastatic lungs immunostained for Gr1 and Tsp-1 showing upregulation of Tsp-1 in lungs from MDA-MB-LM2 tumor-bearing mice treated with DWLPK peptide compared with animals treated with scrambled peptide.

tumors had significantly greater 15-year survival rates and reduced incidence of biochemical failure (Fig. 7B–D). We thus intend to further optimize the Psap-derived peptide as a potential therapeutic agent for advanced metastatic cancer (Fig. 7A).

METHODS

Mice and Cell Lines

All animal work was conducted in accordance with a protocol approved by the Institutional Animal Care and Use Committee. Wild-type C57BL/6J, and GFP transgenic C57BL/6-Tg (*ACTB-EGFP*) 1Osb/J mice were obtained from The Jackson Laboratory. CB-17 SCID mice were obtained from Charles River. Tsp1 knockout mice in the C57BL/6J background, a kind gift from Dr. Shahin Rafii (Weill Cornell Medical College, New York, NY) were bred in the laboratory and genotyped according to standard protocols.

The cell lines PC3 and PC3M-LN4 are previously described (14). Human breast cancer cell lines MDA-MB-231 and MDA-MB-LM2 are described previously (13). The murine Lewis lung carcinoma cell line LLCs/D122 (provided by Lea Eisenbach, Weizmann Institute of Science, Rehovot, Israel) stably expressing RFP and firefly luciferase (1–3), was cultured in Dulbecco's modified Eagle's medium supplemented with 10% FBS. PC3, LN4, and MDA-MB-231 cell lines were obtained from American Type Culture Collection. No authentication of the cell lines was conducted by the authors.

Bone Marrow Isolation and Transplantation

Bone marrow harvest and transplantation were conducted using our published methods (2, 15). BMT was conducted by injecting 5×10^6 total bone marrow cells via tail vein into lethally irradiated (950 rads) 7-week-old C57BL/6 female mice. Bone marrow cells were harvested by flushing femurs and tibias of donor animals including C57BL/6 Tg (*ACTB-EGFP*) 1Osb/J, C57BL/6 WT, or C57BL/6 Tsp-1 knockout mice. After 4 weeks of bone marrow engraftment, reconstitution efficiency was monitored by Western blot analysis of peripheral blood for absence of Tsp-1 protein.

Peptide Generation and Administration

Psap truncation mutants were created by cloning the regions of Psap generated by PCR amplification using the following strategy: saposin A, saposin AB, and saposin ABC were all created using the same 5′ primer: ggcggcgtcgacATGTACGCCCTCTTCCTCC and the following 3′ primers: saposin A: ggcgcctctagaAGAGACTCGCAGAGGTTGAG; saposin AB: ggcgcctctagaACCTCATCACAGAACCC; saposin ABC: ggcgcctctagaGCCAGAGCAGAGGTGCAGC. The PCR products were then cleaved with Xba1 and Sal1 and cloned into pCMVneo.

The *Psap* truncation constructs were then used to transfect PC3M-LN4 using the Fugene6 transfection reagent and protocol (Roche). CM of transfected cells was harvested 48 hours after transfection and used to treat WI-38 lung fibroblasts for 16 hours. After CM treatment, cells were harvested, lysed, and protein expression analyzed by Western blot analysis as previously described (14).

The seven 20-amino acid peptides spanning the length of saposin A were composed of the following sequences:

1–20-SLPCDICKDVVTAAGDMLKD; 11–30-VTAAGDMLKDNATEEEILVY;21–40-NATEEEILVYLEKTCDWLPK;31–50-LEKTCDWLPKPNMSASCKEI; 41–60-PNMSASCKEIVDSYLPVILD; 51–70-VDSYLPVILDIIKGEMSRPG; 61–81-IIKGEMSRPGEVCSALNLCES. All

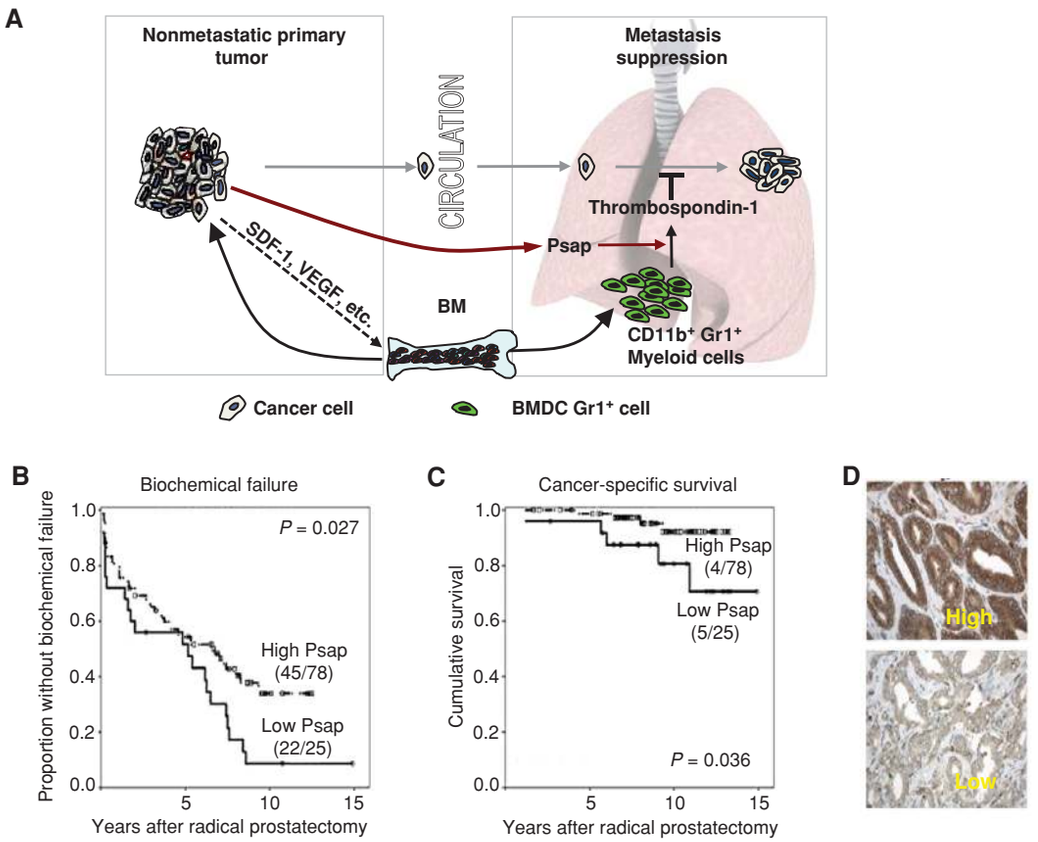

Figure 7. Expression of Psap positively correlates with increased overall survival in prostate cancer. **A,** model showing how metastasis-incompetent primary tumors, by expressing Psap, can systemically generate a metastasis-suppressive microenvironment in the lungs by inducing Tsp-1 expression in the bone marrow–derived $CD11b^+Gr1^+$ myeloid cells. BMDC, bone marrow–derived cells. **B,** immunohistochemical analysis of Psap protein expression in a tissue microarray showing time to biochemical failure in patients with prostate cancer following radical prostatectomy. **C,** immunohistochemical analysis of Psap protein expression in a tissue microarray showing cancer-specific survival in patients with prostate cancer following radical prostatectomy. *P* values indicate significant difference for both endpoints, time to biochemical failure and overall survival ($P = 0.027$ and $P = 0.036$, respectively). **D,** examples of high and low Psap-staining patterns.

peptides were synthesized by Anaspec, Inc. The 13-amino acid cyclic peptide was composed of the following sequence: CDWLPKP-NMSASC.

For *in vitro* analysis of peptide activity WI-38 lung fibroblasts were treated with peptide for 16 hours at a concentration of 5 μg/mL. The cells were then harvested and lysed for Western blot analysis as previously described (14).

The *in vivo* analysis of peptide activity was conducted by treating 8-week-old C57/BL6 mice with 300 μL of PC3M-LN4 CM alone or in combination with peptide, diluted in PBS, at a dose of 30 mg/kg/d via intraperitoneal injection for 4 days. After 4 days, the mice were euthanized by cervical dislocation under isofluorane anesthetic. The lungs were harvested, lysed, and analyzed for protein expression as previously described (14).

For metastasis experiments, the Psap peptide DWLPK and a scrambled peptide LPKDW were synthesized by AnaSpec. Peptide diluted in saline was administered to mice (30 mg/kg) via intraperitoneal injection on a daily basis for 6 days before tumor cell injection and until the end of the metastasis assays.

Conditioned Medium Experiments

PC3 or PC3M-LN4 cells were cultured in RPMI with 10% FBS. A total of 5×10^6 cells were then subcultured in serum-free medium in 10-cm plates for 24 hours to generate CM. Harvested media was centrifuged and filtered through 0.22 μmol/L pore-size filters to remove any cells or cell debris.

WT BMT and *Tsp-1*$^{-/-}$ BMT C57BL/6J mice were pretreated with 200 μL serum-free CM from PC3 or LN4 cells or serum-free RPMI media daily for 6 days via intraperitoneal injection.

Disclosure of Potential Conflicts of Interest

No potential conflicts of interest were disclosed.

Authors' Contributions

Conception and design: R. Catena, K. Gravdal, R.S. Watnick, V. Mittal

Development of methodology: R. Catena, D. Gao, K. Gravdal, L.A. Akslen, R.S. Watnick, V. Mittal

Acquisition of data (provided animals, acquired and managed patients, provided facilities, etc.): R. Catena, N. Bhattacharya, T. El Rayes, S. Wang, H. Choi, D. Bielenberg, S.B. Lee, S.A. Haukaas, K. Gravdal, O.J. Halvorsen, L.A. Akslen, R.S. Watnick

Analysis and interpretation of data (e.g., statistical analysis, biostatistics, computational analysis): R. Catena, N. Bhattacharya, T. El Rayes, S. Wang, S. Ryu, O.J. Halvorsen, L.A. Akslen, R.S. Watnick, V. Mittal

Writing, review, and/or revision of the manuscript: R. Catena, T. El Rayes, H. Choi, S.A. Haukaas, O.J. Halvorsen, L.A. Akslen, R.S. Watnick, V. Mittal
Administrative, technical, or material support (i.e., reporting or organizing data, constructing databases): N. Joshi, O.J. Halvorsen, L.A. Akslen, R.S. Watnick, V. Mittal
Study supervision: R.S. Watnick, V. Mittal

Acknowledgments

The authors thank Bruce Zetter (Children's Hospital, Boston, MA) for comments on the manuscript, and Jenny Xiang of the Genomics Resources Core Facility of Weill Cornell Medical College for the microarray experiments, and Sharrell Lee, Mary Hahn, Gerd Lillian Hallseth, and Bendik Nordanger for technical support.

Grant Support

This study was supported by NIH grant CA135417 (to V. Mittal and R.S. Watnick) and by grants from the Norwegian Cancer Society and the Norwegian Research Council (to L.A. Akslen). This study was also partially supported by the Cornell Center on the Microenvironment and Metastasis through Award Number U54CA143876 from the NCI and Robert I. Goldman Foundation (to V. Mittal) and by the Elsa U. Pardee Foundation and Boston Children's Hospital Technology Development Grant (to R.S. Watnick). R. Catena was supported by fellowships from the "Government of Navarra" and the "Camara Navarra de Comercio" (Navarra, Spain).

Received October 15, 2012; revised February 20, 2013; accepted February 21, 2013; published OnlineFirst April 30, 2013.

REFERENCES

1. Gupta GP, Massague J. Cancer metastasis: building a framework. Cell 2006;127:679–95.
2. Gao D, Nolan DJ, Mellick AS, Bambino K, McDonnell K, Mittal V. Endothelial progenitor cells control the angiogenic switch in mouse lung metastasis. Science 2008;319:195–8.
3. Joyce JA, Pollard JW. Microenvironmental regulation of metastasis. Nat Rev Cancer 2009;9:239–52.
4. Paget S. The distribution of secondary growths in cancer of the breast. 1889. Cancer Metastasis Rev 1989;8:98–101.
5. Psaila B, Lyden D. The metastatic niche: adapting the foreign soil. Nat Rev Cancer 2009;9:285–93.
6. Kaplan RN, Psaila B, Lyden D. Bone marrow cells in the 'pre-metastatic niche': within bone and beyond. Cancer Metastasis Rev 2006;25:521–9.
7. Carlini MJ, De Lorenzo MS, Puricelli L. Cross-talk between tumor cells and the microenvironment at the metastatic niche. Curr Pharm Biotechnol 2011;12:1900–8.
8. Hiratsuka S, Watanabe A, Aburatani H, Maru Y. Tumour-mediated upregulation of chemoattractants and recruitment of myeloid cells predetermines lung metastasis. Nat Cell Biol 2006;8:1369–75.
9. Erler JT, Bennewith KL, Cox TR, Lang G, Bird D, Koong A, et al. Hypoxia-induced lysyl oxidase is a critical mediator of bone marrow cell recruitment to form the premetastatic niche. Cancer Cell 2009;15:35–44.
10. Yan HH, Pickup M, Pang Y, Gorska AE, Li Z, Chytil A, et al. Gr-1+CD11b+ myeloid cells tip the balance of immune protection to tumor promotion in the premetastatic lung. Cancer Res 2010;70:6139–49.
11. Yang L, Huang J, Ren X, Gorska AE, Chytil A, Aakre M, et al. Abrogation of TGF beta signaling in mammary carcinomas recruits Gr-1+CD11b+ myeloid cells that promote metastasis. Cancer Cell 2008;13:23–35.
12. Fridlender ZG, Sun J, Kim S, Kapoor V, Cheng G, Ling L, et al. Polarization of tumor-associated neutrophil phenotype by TGF-beta: "N1" versus "N2" TAN. Cancer Cell 2009;16:183–94.
13. Minn AJ, Gupta GP, Siegel PM, Bos PD, Shu W, Giri DD, et al. Genes that mediate breast cancer metastasis to lung. Nature 2005;436:518–24.
14. Kang SY, Halvorsen OJ, Gravdal K, Bhattacharya N, Lee JM, Liu NW, et al. Prosaposin inhibits tumor metastasis via paracrine and endocrine stimulation of stromal p53 and Tsp-1. Proc Natl Acad Sci U S A 2009;106:12115–20.
15. Nolan DJ, Ciarrocchi A, Mellick AS, Jaggi JS, Bambino K, Gupta S, et al. Bone marrow-derived endothelial progenitor cells are a major determinant of nascent tumor neovascularization. Genes Dev 2007;21:1546–58.
16. Good DJ, Polverini PJ, Rastinejad F, Le Beau MM, Lemons RS, Frazier WA, et al. A tumor suppressor-dependent inhibitor of angiogenesis is immunologically and functionally indistinguishable from a fragment of thrombospondin. Proc Natl Acad Sci U S A 1990;87:6624–8.
17. Lawler J. Thrombospondin-1 as an endogenous inhibitor of angiogenesis and tumor growth. J Cell Mol Med 2002;6:1–12.
18. Starlinger P, Moll HP, Assinger A, Nemeth C, Hoetzenecker K, Gruenberger B, et al. Thrombospondin-1: a unique marker to identify in vitro platelet activation when monitoring in vivo processes. J Thromb Haemost 2010;8:1809–19.
19. Xie L, Duncan MB, Pahler J, Sugimoto H, Martino M, Lively J, et al. Counterbalancing angiogenic regulatory factors control the rate of cancer progression and survival in a stage-specific manner. Proc Natl Acad Sci U S A 2011;108:9939–44.
20. Sund M, Hamano Y, Sugimoto H, Sudhakar A, Soubasakos M, Yerramalla U, et al. Function of endogenous inhibitors of angiogenesis as endothelium-specific tumor suppressors. Proc Natl Acad Sci U S A 2005;102:2934–9.
21. Jimenez B, Volpert OV, Crawford SE, Febbraio M, Silverstein RL, Bouck N. Signals leading to apoptosis-dependent inhibition of neovascularization by thrombospondin-1. Nat Med 2000;6:41–8.
22. Reiher FK, Volpert OV, Jimenez B, Crawford SE, Dinney CP, Henkin J, et al. Inhibition of tumor growth by systemic treatment with thrombospondin-1 peptide mimetics. Int J Cancer 2002;98:682–9.
23. Raugi GJ, Mumby SM, Abbott_Brown D, Bornstein P. Thrombospondin: synthesis and secretion by cells in culture. J Cell Biol 1982;95:351–4.
24. Ebbinghaus S, Hussain M, Tannir N, Gordon M, Desai AA, Knight RA, et al. Phase 2 study of ABT-510 in patients with previously untreated advanced renal cell carcinoma. Clin Cancer Res 2007;13:6689–95.
25. Markovic SN, Suman VJ, Rao RA, Ingle JN, Kaur JS, Erickson LA, et al. A phase II study of ABT-510 (thrombospondin-1 analog) for the treatment of metastatic melanoma. Am J Clin Oncol 2007;30:303–9.
26. Ahn VE, Leyko P, Alattia JR, Chen L, Privé GG. Crystal structures of saposins A and C. Protein Sci 2006;15:1849–57.
27. Shevde LA, Welch DR. Metastasis suppressor pathways–an evolving paradigm. Cancer Lett 2003;198:1–20.
28. Cook LM, Hurst DR, Welch DR. Metastasis suppressors and the tumor microenvironment. Semin Cancer Biol 2011;21:113–22.
29. Jaffe EA, Ruggiero JT, Falcone DJ. Monocytes and macrophages synthesize and secrete thrombospondin. Blood 1985;65:79–84.
30. DiPietro LA, Polverini PJ. Angiogenic macrophages produce the angiogenic inhibitor thrombospondin 1. Am J Pathol 1993;143:678–84.
31. Gao D, Joshi N, Choi H, Ryu S, Hahn M, Catena R, et al. Myeloid progenitor cells in the premetastatic lung promote metastases by inducing mesenchymal to epithelial transition. Cancer Res 2012;72:1384–94.
32. Fidler IJ. The organ microenvironment and cancer metastasis. Differentiation 2002;70:498–505.